

Submerge: Visualizing Storm Surge Flooding Simulations in Immersive Display Ecologies

Saeed Boorboor, Yoonsang Kim, Ping Hu, Josef M. Moses, Brian A. Colle,
and Arie E. Kaufman, *Fellow, IEEE*

Abstract—We present *Submerge*, an end-to-end framework for visualizing flooding scenarios on large and immersive display ecologies. Specifically, we reconstruct a surface mesh from input flood simulation data and generate a to-scale 3D virtual scene by incorporating geographical data such as terrain, textures, buildings, and additional scene objects. To optimize computation and memory performance for large simulation datasets, we discretize the data on an adaptive grid using dynamic quadrees and support level-of-detail based rendering. Moreover, to provide a perception of flooding direction for a time instance, we animate the surface mesh by synthesizing water waves. As interaction is key for effective decision-making and analysis, we introduce two novel techniques for flood visualization in immersive systems: (1) an automatic scene-navigation method using optimal camera viewpoints generated for marked points-of-interest based on the display layout, and (2) an AR-based focus+context technique using an auxiliary display system. *Submerge* is developed in collaboration between computer scientists and atmospheric scientists. We evaluate the effectiveness of our system and application by conducting workshops with emergency managers, domain experts, and concerned stakeholders in the Stony Brook Reality Deck, an immersive gigapixel facility, to visualize a superstorm flooding scenario in New York City.

Index Terms—Immersive visualization, Flooding simulation, Camera navigation, Mixed Reality.

1 INTRODUCTION

THE increase in extreme weather events [1] has led to a growing need for visualization systems that can aid scientists, emergency managers, and concerned stakeholders to effectively prepare for the impacts of potential catastrophic events. Of particular concern is coastal and inland flooding. Studies have shown that floods account for 43% of all disasters and are the most frequently occurring natural disasters worldwide [2]. Although there have been advances in weather forecasting models, its usefulness depends greatly on the human decision-making dimension [3].

Predicted flooding scenarios using numerical simulation models are typically rendered as 2D visualizations superimposed onto 2D maps. While a 2D representation can convey the birds-eye view extents of the flooding, it relies on the user to perceive depth information based on cues such as color. Extending the visualizations to 3D [4], [5] enhances the user's understanding of flooding depth, intensity, and impact with respect to its spatial surroundings. However, when analyzing a vast virtual scene at a high level-of-detail (LoD), the limited field-of-view (FoV) of a single-screen desktop workstation can impel a user to engage in frequent pan-and-zoom interactions. This has motivated us to develop *Submerge*, an application and system for flood visualization that harnesses the screen real-estate and visual acuity of large immersive visualization systems.

Specifically for scientific analysis, large, high-resolution displays, such as CAVEs and immersive tiled displays

have been shown to improve user performance in various visualization tasks [6], [7], [8]. In essence, utilizing large screen real-estate allows for a wider FoV. This is particularly beneficial for applications such as flood visualization, where immediate access to local and global data context is vital for well-rounded analysis and decision-making. Moreover, leveraging high-resolution graphics and high-performance capabilities of such facilities enhances the detail and granularity of information as well as the realism of the visualizations, which has been shown to positively influence perceptions and behaviors in preparing for and responding to natural hazards [9].

Submerge addresses three important design challenges. First, visualizing simulation data coupled with elements of a geographic information system (GIS) requires constructing and rendering large 3D meshes from data arranged on structured and unstructured grids. Thus, a system infrastructure with low latency and real-time synchronization across display nodes is required for effective interactivity. To this end, we have developed *Submerge* as a modular and scalable system that abstracts visualization design at an application level from its deployment across a multi-node multi-display system. By providing the layout and cluster configuration of a display system, *Submerge* determines appropriate camera projections for each physical display in the setup, along with view-dependent data extents for rendering the virtual scene. At the application level, we render the simulated flood as a 3D surface mesh with propagating waves to visualize flow direction. To optimize computation time and memory, and to support LoD rendering, we achieve this by representing the simulation data on an adaptive heightfield grid [4], [10] using a dynamic quadtree datastructure.

Second, flood visualization applications require frequent data interaction. Unlike a desktop setup, where applications

- Boorboor, Kim, Hu, and Kaufman are with the Department of Computer Science, Stony Brook University.
E-mail: {sboorboor, yoonsakim, pihu, ari}@cs.stonybrook.edu.
- Moses and Colle are with the School of Marine and Atmospheric Sciences, Stony Brook University.

Manuscript received xxxxx; revised xxxxx.

have a graphical user interface and users have access to input devices, interaction in immersive settings usually adopts a natural mode, such as walking and hand gestures, and occasionally by using hand-held controllers. To allow user-interface controls, Submerge provides a unique focus-and-context interaction by integrating a video see-through augmented-reality (AR) auxiliary display to the immersive setup. In integrating a hand-held device as an auxiliary display, Submerge enables augmenting additional information and visualizations atop the surrounding displays, facilitating local contextual analysis while simultaneously having access to global data. Moreover, to ensure an interactive user experience, we have included a remote rendering protocol in Submerge that offloads computation and rendering tasks from the auxiliary device to a server.

Finally, effective navigation is an essential element for gaining a complete understanding of the scene. This becomes additionally challenging for large and cluttered scenes, where multiple points-of-interest (POIs) have to be observed. Determining appropriate views and designing methods for navigation in immersive systems is an active ongoing area of research [11]. To this end, we have developed an optimal camera view-finding algorithm that maximizes view coverage of user-defined POIs based on the layout of the display system. Using the camera views, we additionally facilitate scene navigation by determining a camera path that smoothly transitions along subsequent viewpoints by connecting them using straight lines and quadratic Bézier curves such that it avoids collision with 3D scene objects, minimizes motion sickness for immersive environments [12], and maintains a camera look-at vector in the direction of the shoreline to ensure visibility of the coastal and inland flooding.

Submerge is developed as a collaboration between computer scientists and atmospheric scientists and feedback from flood managers. In this paper, we demonstrate the visualization of a flooding scenario in New York City (NYC) and deploy it on the Stony Brook University Reality Deck (RD), the largest immersive gigapixel display facility in the world [13]. We evaluate our system based on feedback from workshops conducted with the NYC flood managers, meteorologists, domain scientists, graduate students in atmospheric sciences, and other stakeholders.

We summarize our contributions as follows:

- An end-to-end scalable and modular system designed specifically for visualizing flooding data on large immersive display setups.
- An AR-based auxiliary display medium for focus+context visualization in immersive settings.
- A novel automatic camera viewpoint finding algorithm that facilitates effective scene exploration.

2 RELATED WORKS

Visualization of Flooding Simulation Data: Tools for visualizing flooding scenarios generally feature a geographical map interface embedded with rasterized information from numerical simulation models [14], [15], [16]. However, it has been shown that 2D representation of flooding data

limits the full spectrum perception of additional multivariate geospatial attributes [17], and can lead to the lack of understanding of the severity and ineffective preparation for flooding scenarios [9]. In integrating flood data with 3D objects, Cornel et al. [4] have developed visual encodings on 3D SCENE objects, establishing an intuitive relation between objects and flooding events information. To fully integrate geospatial attributes such as terrains, Cornel et al. [5] have developed fast interpolation of adaptive grids to reconstruct a surface mesh. Additionally, they present an algorithm for realistic water shading with depth perception cues. In Submerge, we derive our mesh interpolation and wave synthesis techniques from Cornel et al. [5] and expand it to adapt to distributed visualization systems and immersive settings. Particular to the VR domain, several game applications exist for training and behavior analysis in the event of flooding [18], [19], and to aid non-scientific stakeholders in visualizing and understanding flood simulation data without prior technical knowledge [20]. In contrast, Submerge provides a more wholesome framework for VR by presenting a novel interaction interface for collaborative spaces, and camera view-finding and path-planning algorithms specific to the domain requirements.

Interaction in Immersive Systems: Large display systems pose two important challenges for data interactivity: (1) individual-level exploration of the data visualized collectively with other users, and (2) implementing scalable interaction metaphors. Reipschlag et al. [21] have addressed the former by utilizing an AR head-mounted display (HMD) device to provide analytical information on top of the visualization being presented. Chen et al. [22] have developed a system that supports the independent exploration of global data using a smartphone. Beyond the screen space, Nishimoto and Johnson [23] have developed a method to extend a user's field of regard by displaying additional information using an AR HMD. For the latter, the most widely adopted technique has been to utilize tracking hardware in the display facility to translate human gestures into interaction [24], [25], [26]. Another interaction metaphor, using a touch-enabled surfaces, have been used to interact with the data directly [27], [28], [29]. Recent works have investigated the use of commodity hardware for interaction. Siddhpuria et al. [30] have explored the use of a personal smart device as a pointing device. Babic et al. [31] leveraged off-the-shelf smartphone cameras for hand, head, body, and gaze tracking to interact with a distant display. Particularly for large display systems, Langner and Dachsel [32] have developed a system to use spatially-aware mobile devices in tiled-display ecology. Chen et al. [22] have introduced a unique method of interaction whereby a user takes a photograph of the display using a mobile device and subsequently uses the photo to explore, edit, and navigate the device. In contrast to existing works presented, our auxiliary display system combines components of exploration, extended visualization, as well as interaction using a novel framework that utilizes AR to seamlessly bridge interaction metaphors between the physical world and virtual scene.

View-finding and Path-Planning: Early on, Kamada and Kawai [33] have formulated rules for determining a good view of basic shapes by maximizing the projection of lines on the objects. We refer the reader to a comprehensive

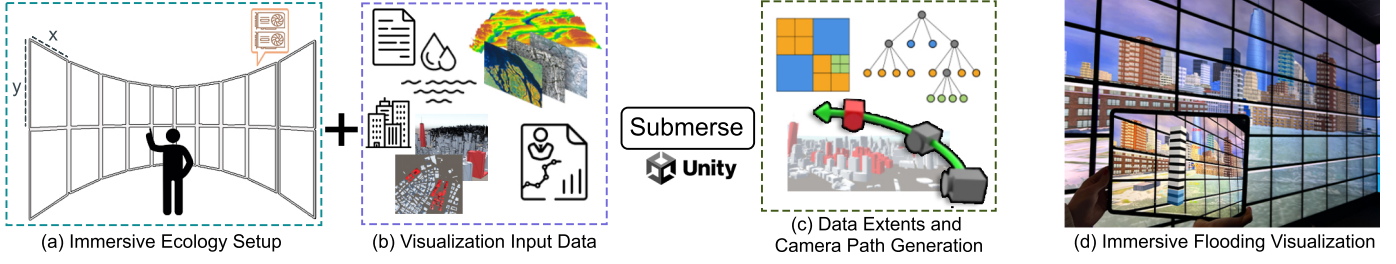


Fig. 1. For a defined display system (a) and input flooding and GIS data (b), Submerge manages data extents and generates automatic camera viewpoints and navigation trajectory (c) to render 3D immersive visualization of the flooding scenario (d).

review by Bonaventura et al. [11] on viewpoint selection methods for polygonal data. More recently, information entropy [34] has been considered a measure for determining visible information. Arbel et al. [35] have formulated view selection based on Shannon entropy maps by measuring object recognition in a monochrome view. Vázquez et al. [36] modeled view selection as an object visibility maximization problem. Specific to landscape scenes, Stoev et al. [37] have developed a method for automatic camera positioning for terrain datasets by maximizing scene depth and the projected area. In terms of navigation, Huang et al. [38] have introduced a camera motion design method, particularly for urban scenes. Given a set of viewpoints, a path is determined by their interests according to the number and the shapes of the visible buildings. Furthermore, Lin et al. [39] have developed a framework for large-scale scene data perception and reconstruction. In contrast to existing works, our view-finding algorithm is two-fold: determining a view that maximizes information visibility and also integrates the surrounding information and display configuration in its formulation. Based on the viewpoints, we develop a camera path control method for large-scale visualization, also taking into consideration the domain information.

3 DOMAIN BACKGROUND AND REQUIREMENTS

Understanding and analyzing numerical models that describe and predict real-life environment around us makes atmospheric science a very visual field. While data collection methods and forecasting models have become better and more sophisticated, tools for their visualization are still primarily based on 2D projections and limited to pan-and-zoom interactions. To effectively use data for studying unprecedented weather extremes from climate change, as well as for collaborating with stakeholders to plan resilience measures, Submerge has been designed and developed based on the following requirements identified by domain experts:

R1 – 3D visualization of flooding scenarios: To better understand the flooding intensity, a visualization system is needed to stimulate a realistic perception of the flooding depth and severity with respect to its geographic surroundings and progression over time.

R2 – A collaborative space for diverse stakeholders: A method to facilitate a fully integrative and collaborative space for stakeholders, such that users can experience a shared understanding as well as interact independently with the scientific findings of the climate catastrophe.

R3 – Optimizing POI views and navigation in large scenes: One of the challenges of 3D visualization is scene

navigation and adjusting the camera to achieve good views, especially in large urban scenes. To this end, for a set of input POIs, the system should assist with providing effective views for analyzing the progression of coastal flooding with minimal viewing occlusion. For a collection of POIs, the system should aid in navigating the scene.

4 SUBMERSE

Based on the domain requirements, we have designed Submerge as an application and system to visualize storm surge flooding simulations by specifically utilizing immersive display facilities. Fig. 1 provides an overview of Submerge application and system pipeline.

For an input simulation data, we present an interactive visualization of the flooding scenario by integrating the flooding level into a to-scale 3D virtual model of the corresponding geographic area (**R1**). The virtual scene is set up using GIS data, such as digital elevation map (DEM) and satellite imagery, and supplementary scene objects, such as 3D buildings and reference 3D objects. We describe our method for the processing of the input simulation data to reconstruct an animated water surface, visualizing the flooding level and direction, in Sec. 4.1.

High-resolution display facilities such as CAVEs and immersive tiled-displays have been shown to enhance data realism and allow a more effective exploration of three- and higher-dimensional data by tapping into the human peripheral vision [8] (**R1**). Moreover, these visualization systems, depending on the layout, present a natural space for multi-user collaboration and interaction (**R2**). In Sec. 4.2, we present the Submerge system design which enables the deployment of the visualization application to a multi-node, multi-GPU display facility. Specifically, based on the configuration and geometry of a display setup, Submerge manages synchronized instances of the application for each viewport in the system and optimizes computational and memory resources by determining view-dependent data extents. Additionally, we have developed a novel AR-based auxiliary interaction method for immersive facilities, which we describe in Sec. 4.3. Using an auxiliary display device, Submerge enables users to perform localized visual analytics seamlessly atop the displayed visualization (**R2**).

Finally, to facilitate an effective exploration of large scenes (**R3**), we have designed an energy function that automatically generates optimal camera viewpoints for user-defined POIs, based on parameters such as the visualization display layout, POI visibility, and the distance from the

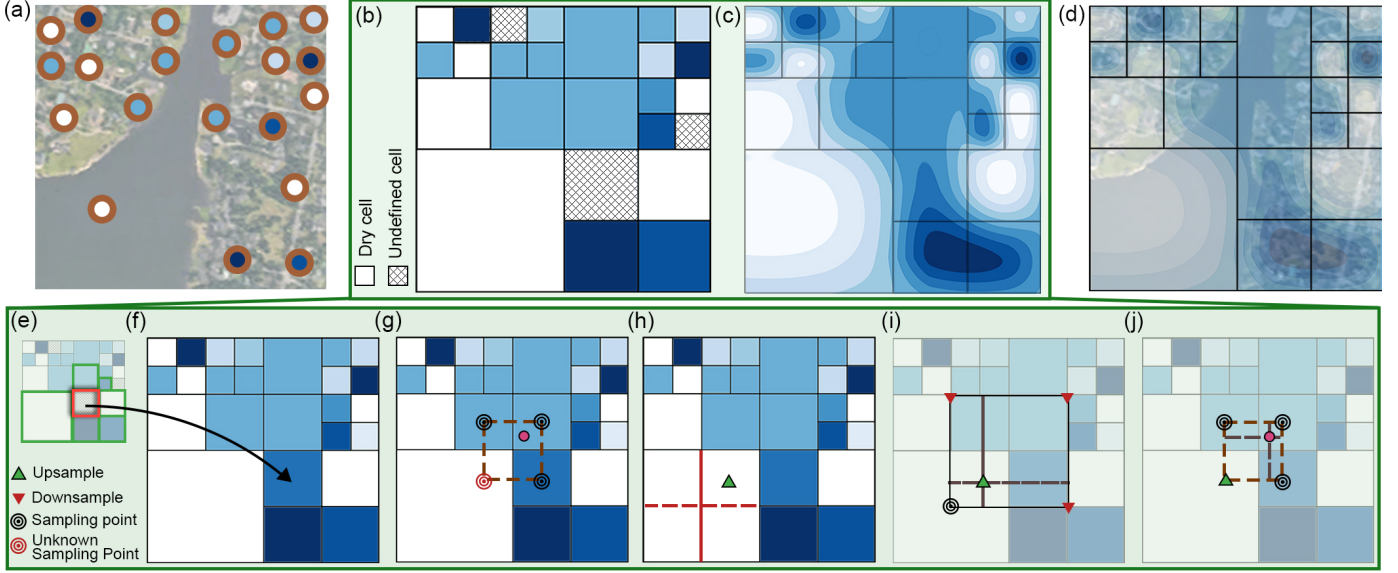


Fig. 2. An example of constructing a water surface mesh using an adaptive grid. For flood datapoints defined on a geographic location (a), we discretize the data on a quadtree (b) and interpolate the values to construct a smooth and continuous field as shown in (c) and (d). A cell without a datapoint (e) is defined by averaging the values of its neighboring defined cells (f). To interpolate a value for the red point in (g), we apply bilinear interpolation on the cells that bound the point. However, since one of the sampling cells, marked in red, has a lower cell resolution, we divide the cell (h) and assign a value by upsampling. The upsampling is done by applying bilinear interpolation on the neighboring same-resolution cells (i). A lower resolution value is calculated using downsampling, that is, the average value of all its child higher resolution cells. Finally, a value for the point is constructed by applying bilinear interpolation on the same-resolution cells (j).

user. Using the set of calculated viewpoints, we generate a smooth camera path for navigating to the POI views. Our camera path algorithm is designed to avoid occlusion with scene objects during navigation and aims to minimize sickness due to motion in immersive settings. The camera view-finding optimization function and path generation algorithm are presented in Sec. 4.4.

4.1 Flood Simulation Rendering

The flood simulation data, which serves as input to our application, is a time series data of scalar water elevation values and 2D tidal velocity, discretized over a vast irregular grid of latitude and longitude positions.

4.1.1 Quadtree-based Height-Field Reconstruction

Although using a high-resolution grid is desirable for generating a smooth and continuous surface, it has a high memory and performance overhead with increasing spatial extents. To this end, we adopt adaptive height-field grid which is a discretized representation of data on an unstructured grid of varying cell sizes [40]. By interpolating cell-centered values on the grid, a surface mesh can be reconstructed for a particular resolution level. Fig. 2 illustrates how this process is applied to our application. For a collection of water elevation datapoints, shown in Fig. 2(a), we discretize the data using a quadtree datastructure, as shown in Fig. 2(b). The main advantage of using a quadtree is its low memory footprint, which is particularly important for limited GPU memory, as well as its hierarchical data representation, which enables LoD rendering. Each leaf node in the quadtree corresponds to a cell of the height-field grid, and the value of each cell, illustrated using shades of blue in Fig. 2(b), is defined using the datapoint value

bounded by the leaf node. To enable LoD rendering, we assign parent nodes to have a value equal to the average value of their children. Finally, using a regular triangular mesh, we render a water surface where the height of each vertex is determined by applying 2D bilinear interpolation on the four cells that enclose the vertex. A planar result of the interpolated values is shown in Fig. 2(c).

Notice in Fig. 2(b) that in sub-dividing a quadtree node, a child node may not contain a datapoint, resulting in an *undefined* value in the height-field cell. Moreover, the simulation output can also have *dry* datapoints, that is, the spatial location does not flood for certain timepoints, and in some cases, the entire duration of the simulated flood (this is specifically to define a boundary for inland spatial locations beyond which no flooding occurs). For dry cells, we use the average height of the underlying terrain obtained from the input DEM, whereas for the undefined cells, we assign an average value of all the defined cells in the neighborhood.

To correctly interpolate height values from varying cell sizes, we modify the adaptive reconstruction introduced by Cornel et al. [4]. In their method, if a neighboring cell is of a different size, an imaginary cell with an equivalent size is reconstructed by upsampling (for a higher resolution level) or downsampling (for a lower resolution level). In our variation, the downsampled value is simply the averaged value assigned to the corresponding node's parent, as in our quadtree reconstruction above. To reconstruct an upsampled value, a similar 2D bilinear interpolation is applied using the lower resolution values of the four bounding cells. Fig. 2(e)-(f) shows this process schematic representation. One caveat to this approach is that the cell neighbors can differ by, at most, one level of resolution. We implement this constraint in our quadtree construction step.

We furthermore extend this technique to facilitate

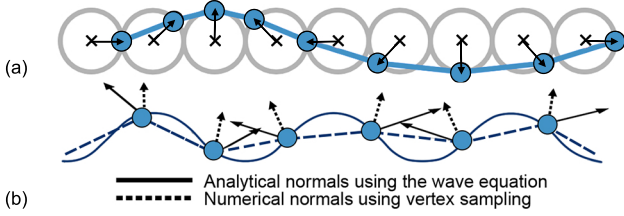


Fig. 3. (a) shows vertex motion following a Gerstner wave and (b) illustrates the difference in calculating analytical and mesh normals.

LoD rendering. Although the hierarchical datastructure of quadtrees supports LoD by design, we restrict the lowest renderable resolution of a sub-tree to be the node whose children belong to the same type, that is, all four children should either be flooded or dry. This condition prevents dry cells from being incorrectly estimated to have flooding. Note that for leaf nodes that correspond to undefined cells, their extrapolated flooding value is used to propagate to the parent node, thus categorizing it as a flooded node.

4.1.2 Flooding Direction Visualization

To visualize tasks that have a behavioral attribute of flow, for instance, inundation, information cannot be perceived by observing a static mesh. This becomes particularly true when time-series data is visualized while paused for a single instance. A natural instinct then is to repetitively toggle back and forth to observe change and variation. Moreover, visual metaphors such as glyphs may add to the complexity of the visualization [4], especially amongst diverse stakeholders.

To enable an intuitive perception of flow for a single timepoint, we animate the water to emulate wind-driven surface waves. Typically in computer graphics, realistic waves are synthesized using the Navier-Stokes equation. However, for a more efficient and simplified approach, we apply Gerstner wave synthesis model [41] using velocity vectors from the simulation data. Gerstner waves produce nearly realistic-looking waves based on a fundamental observation that, unlike a particle system where particles move with the wave, mesh vertices can be displaced along a trochoidal function. Specifically, as the crest of a wave approaches, in addition to being vertical displacement defined by a sine function, a point moves horizontally towards the direction of the crest to simulate the phenomenon of water particles filling up the space under the crest. Conversely, as the crest passes, the point slides back to its resting position on the horizontal axis. A schematic representation of this displacement is shown in Fig. 3.

For a vertex point $P_{xyz} = (x, y, z)$ on a surface mesh, its displacement along a Gerstner wave is calculated as follows:

$$W(P_{xyz}, \vec{v}, \lambda, t) = \begin{cases} P_{xy} + \frac{s}{k} \cos(kD - ct) & \text{for } (x, y) \\ P_z + \frac{s}{k} \sin(kD - ct) & \text{for } z \end{cases} \quad (1)$$

$$k = \frac{2\pi}{\lambda}, \quad D = P_{xy} \cdot \vec{v}, \quad c = \sqrt{\frac{g}{k}} \quad (2)$$

where λ is the wavelength, g is gravity, \vec{v} is the 2D unit vector of the simulation tidal velocity, s is a defined wave steepness parameter, and t is the animation time interval.

Directly sampling wave orientations from the corresponding quadnodes result in tiling artifacts. Moreover, rendering a single uniform train of waves traveling across the water surface presents a non-realistic feature. Existing works have suggested superimposing multiple waves sampled from increasing spatial extents, especially for open water bodies [41], [42]. This not only maintains a degree of realism but also allows the visualization of a regional principal flow as well as local flow direction.

In our implementation, we use the overlapping bounds suggested by Cornel et al. [4]. An imaginary tile, T around P_{xy} , for a spatial extent spanning λ , is defined as $T = [x_0, x_1] \times [y_0, y_1]$, where

$$(x_0, y_0) = 2\lambda \left\lfloor \frac{(x, y)}{2\lambda} \right\rfloor, \quad (x_1, y_1) = (x_0, y_0) + (2\lambda, 2\lambda) \quad (3)$$

A wave for T is then calculated using its center position and an average tidal direction, sampled from each of its four corners. To get an overlapping region, T is then shifted horizontally and vertically by λ such that the centers of the four tiles $[T, T + (\pm\lambda, 0), T + (0, \pm\lambda), T + (\pm\lambda, \pm\lambda)]$ enclose P_{xy} in a box of length λ . Thus, a wave W_λ for P_{xy} is calculated as the waves bilinear interpolation at each tile center, using the following horizontal and vertical weights:

$$\alpha = \frac{1}{2} - \frac{1}{2} \cos\left(\frac{\Delta x}{2\lambda}\right), \quad \beta = \frac{1}{2} - \frac{1}{2} \cos\left(\frac{\Delta y}{2\lambda}\right) \quad (4)$$

where Δx and Δy are the distance of P_{xy} along the x and y directions with respect to the tile centers. For superimposing multiple waves of increasing spatial extents, waves for n different wavelengths are generated using $\lambda_i = r_i 2^i \lambda_0$, where λ_0 is the shortest considered wavelength and $r_i \in [0.8, 1.0]$ is a random value to avoid frequency doubling. The final vertex displacement is determined using:

$$W = W_{\lambda_0} + \sum_{i=1}^n W_{\lambda_i} \quad (5)$$

Since the waves are generated on a triangular mesh with discrete intervals, we use analytical normals instead of vertex normals for continuous lighting and shadow effects (see Fig. 3 for this comparison). The normal \vec{n} for each vertex is the spatial derivative of Eq. 1:

$$\vec{n} = \begin{bmatrix} 1 - D_x^2 s \sin f \\ D_x s \cos f \\ -D_x D_z s \sin f \end{bmatrix} \times \begin{bmatrix} -D_x D_z s \sin f \\ D_z s \cos f \\ 1 - D_z^2 s \sin f \end{bmatrix} \quad (6)$$

Finally, we address two implementation details. First, an averaged neighborhood tidal velocity is assigned to an *undefined* node, however since *dry* nodes do not have tidal velocities, we set $W_{\lambda_0} = 0$. Second, to reduce loss of tidal direction due to averaging, we impose a further constraint for determining the lowest resolution LoD subtree, such that the angles between all pair-wise unit vectors of the subtree children should not exceed 15° .

4.2 Immersive Display System

Submerge is intended to be generalized for any display layout and configuration – a single desktop to a large and immersive setup, a single node to a multi-node, multi-GPU configuration. For an input display setup, we (1) determine

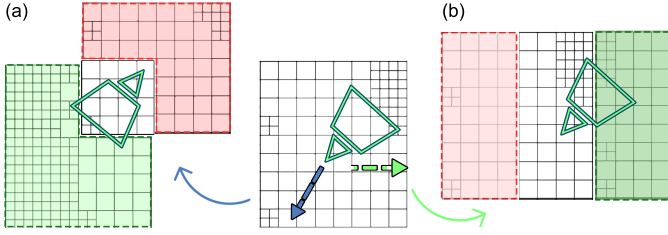


Fig. 4. Two examples (a) and (b) of our dynamic quadtree update based on camera motion. Red represents the deleted quadrants and the newly added nodes are shaded in green.

the scene data extents for each display and use dynamic quadrees to allow interactive data update (Sec. 4.2.1), (2) set up a localization and rendering protocol for the auxiliary display (Sec. 4.3), and (3) configure optimal camera views for marked POIs (Sec. 4.4).

A display system is defined using the position, orientation, and dimensions of each screen in the layout, along with a *head* position. The *head* is primarily a reference point that represents a unified position of the display system in the virtual scene and is used to calculate the camera projection matrix for each display. At a systems level, Submerse is designed as a client-server architecture, where the server manages scene synchronization and sends interaction commands across the client (display) nodes.

4.2.1 Data Extents and Scene Update

To optimize data retrieval, we have designed our quadtree to contain data for spatial bounds proportional to the display’s viewing frustum, which is dynamically updated during scene navigation. Specifically, the bounds of a quadtree are initialized such that the virtual position of the display lies in the center of the quadtree and it spans the maximum horizontal extents of the camera-view frustum pyramid + a buffer region. The camera view frustum for a screen is determined using its dimensions, relative position from the *head*, and camera parameters.

For maintaining an interactive framerate during scene exploration, we have designed the first-level quadrants of the quadtree (children of the root node) to be dynamic. That is, the quadrants are selectively updated based on the camera movement direction. By tracking the displacement of the physical screen in the virtual scene, we determine which quadrant needs to be updated as the screen approaches the quadtree outer boundary. Consequently, instead of constructing an entire quadtree with new spatial extents, we discard the quadrants that are beyond a threshold distance from the screen position, rearrange the pointers of the preserved quadrants to reflect the new root bounds, and populate nodes for the new quadrants. In Fig. 4, we illustrate this process using two examples of camera movement. In our implementation, the quadnode updates are performed in parallel using multi-threading and are either triggered as the user manually navigates through the virtual scene or scheduled sequentially based on a predefined camera path generated using our algorithm described in Sec. 4.4.

4.3 Auxiliary Display

To support the analysis and decision-making of large datasets, visualization applications typically provide users with tools that can systematically present a global overview of the data as well as a detailed depiction of a selected local area. Naturally, large and immersive display facilities are most functional when it comes to projecting vast extents of global data, compared to personalized display screens and desktop setups. However, the larger the screen real-estate, the more challenging it becomes to design tools for localized visualization. To this end, we have designed a novel mixed-reality focus+context technique where the global data is projected on the surrounding immersive display facility while the localized contextual visualizations are shown on a hand-held AR-enabled device (which we term an auxiliary display in the Submerse system).

4.3.1 Device Setup

The seamless integration of an auxiliary display into an immersive display system requires tracking and localization in both the physical space and the virtual world. In other words, specifically for immersive facilities, the auxiliary system must accommodate two domains: the user’s physical movements, including device orientation, and the position of the virtual camera in the virtual scene. For localization in the physical space, we leverage recent advances in AR that effectively maps the position of a device in real-time. Using the defined *head* position, we are able to determine the physical-to-virtual space transformation of the auxiliary device. Since the server node is responsible for the data, scene, and interaction synchronization in the system workflow, the auxiliary device is likewise connected to the server, which solves for the physical-to-virtual transformation and determines the visualizations that need to be rendered on the auxiliary display. Fig. 5 presents a schematic representation of the system protocol.

Here we address an important challenge related to AR-based rendering of the visualizations on the auxiliary display. Unlike typical AR applications that render virtual objects onto the physical world, we render virtual objects that are meant to be augmented onto a scene defined by a virtual world, displayed on a physical plane (screens). This mapping introduces scale disparities since two cameras are involved, the auxiliary display camera and the Submerse virtual camera. To solve this mapping, we utilize render textures on the server. First, based on the device localization, the required visualizations, such as the dip-stick or custom data visualizations shown in Fig. 5, are rendered in an empty virtual scene with extents similar to the flooding scene. Next, we use the Submerse camera parameters to bake a view of the rendered visualization onto a virtual texture that replicates the size and layout of the display facility. Thus, instead of rendering virtual objects from the scene, the auxiliary display rasterizes the visible parts of the render texture based on the device camera parameters.

One final matter in the system workflow deserves attention. Given the limited GPU and compute resources of a mobile device, user experience can be significantly affected when rendering complex scenes and managing large datasets. To offload this burden from the auxiliary device,

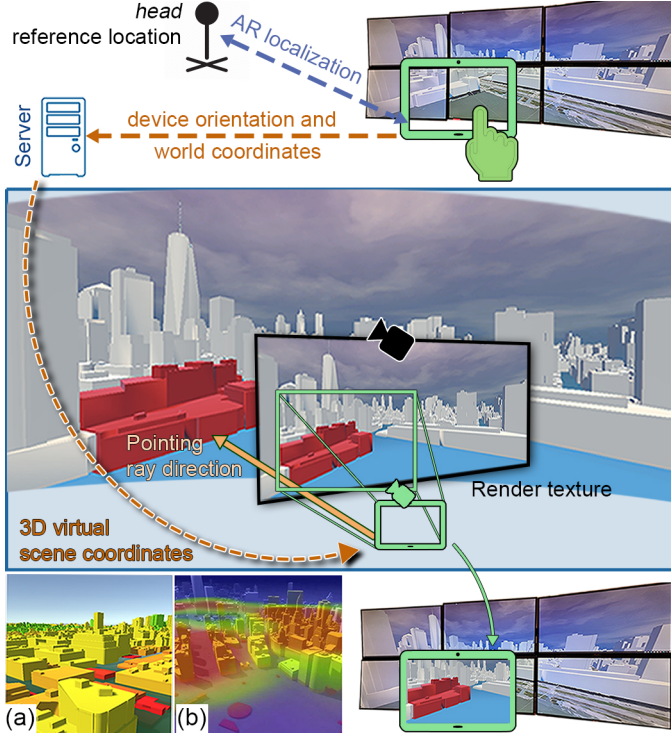


Fig. 5. System protocol of our AR-based auxiliary display. (a) and (b) are two example applications that show the flooding level with respect to building height (on a diverging color map of green to yellow to red, with red being most severe) and a heatmap of population density, respectively.

we have implemented a web-based remote rendering module into our system. As a result, the rendering is performed on the server and the final result is a series of textures received by the device over the network.

4.4 Camera View Finding and Navigation Trajectory

We have designed an automatic camera viewpoint-finding algorithm based on factors that maximize POI visibility with respect to the virtual scene and physical display layout. Below, we describe each term of our objective function, followed by an algorithm we have designed for refining the optimal views based on user-defined thresholds and generating a path for navigating through the viewpoints. Mathematically, a POI is defined using its 3D position and a scalar value indicating its expansion radius, and a camera viewpoint, v is defined using its 3D position, and yaw and pitch angles. For all the terms described below, E_X is a large-valued penalty score to constrain the system to satisfy the respective user-defined threshold value or condition.

View coverage: To anchor a POI in the center of the camera view frustum, we define the term view coverage, $R(v)$ as the combination of the eccentricity of a POI's projection on the camera view, $H_e(v)$, and the alignment between the camera up vector and v , denoted as $H_u(v)$:

$$R(v) = \begin{cases} E_R, & \text{if } a_p > A_p \\ \omega_u \left\| \frac{2a_p}{\pi} \right\|^2 - (\vec{p}\vec{q} \cdot \vec{d}), & \text{otherwise} \end{cases} \quad (7)$$

where ω_u is a weight to control the relative influence between eccentricity and viewing direction alignment, a_p is

the pitch angle of the camera pose, p and q are the positions of the camera and POI respectively, \vec{d} is the camera look-at direction, and $A_p \in [0, \pi/2]$ is a user-defined maximum allowable pitch angle for the camera.

POI visibility: To ensure effective visibility of a POI, we penalize a candidate view where the POI is occluded by a building, scene object, or another POI using:

$$O(v) = \begin{cases} E_O, & \text{if this POI is occluded} \\ 0, & \text{otherwise} \end{cases} \quad (8)$$

We use a discretized visibility grid to efficiently check if the POI is occluded by any cell when projected onto the camera view. A cell in the visibility grid is defined using a cuboid with a height equal to the maximum height of the 3D objects occupying the cell bounds (except the water mesh). Moreover, we define an additional term $D(v)$ to control the closeness of the POI to the display:

$$D(v) = \begin{cases} E_D, & \text{if } \frac{\|q-p\|^2}{k} > K \\ \frac{\|q-p\|^2}{k}, & \text{otherwise} \end{cases} \quad (9)$$

where k is a constant to normalize the distance calculate and K is the user-defined maximum allowable distance of the POI from the camera.

Coastal vicinity: Often, for POIs on the coastline, it is preferred that the camera view is in the direction of shore-to-POI, so that the effect of the progression of the coastal flood approaching the POI may be observed. To this end, we model this preference as location preference $L(v)$.

$$L(v) = \begin{cases} 0, & \text{if in offshore locations on map} \\ E_L, & \text{otherwise} \end{cases} \quad (10)$$

Final objective: Thus, to find a set of optimal viewpoints, C , for M POIs, we define the following objective function with customizable weights:

$$C = \operatorname{argmin} E(v) \quad (11)$$

$$E(v) = \sum_{i=1}^M (\Omega + R_i(v) + \omega_o O_i(v) + \omega_d D_i(v) + \omega_l L_i(v)) \quad (12)$$

We empirically determine the weights to be $\omega_u = 0.5$, $\Omega = 10.0$, $\omega_o = 1.0$, $\omega_d = 1.0$, $\omega_l = 0.50$ and the penalties $E_X = 100.0$. For N displays, the total objective is calculated as:

$$E(v) = \sum_{i=1}^N \sum_{j=1}^{N'} E_i(v_j) \quad N' = \{x \in N \mid x \neq i\} \quad (13)$$

Eq. 13 additionally accumulates a score for all remaining displays in the layout by rotating a candidate camera viewpoint v , along its look-up axis, with the relative yaw angle between the display pairs. This allows us to obtain a set of minimum camera viewpoints for multiple POIs based on the display layout. We further demonstrate this using 2 layouts in our results presented in Sec. 6.

The arbitrary terrain elevation and building heights create a complex search space for resolving a minima since the derivative of a sample point contributes little to locating an optimal candidate. Therefore, we chose Particle Swarm Optimization (PSO) [43], a derivative-free optimization method

that does not depend on a sampled gradient or covariance matrix of the sample set, to find a set of optimal viewpoints with minimum objective function score.

Given a set of viewpoints next we calculate the transition trajectory between viewpoints pairs. A straight line segment is preferred for connecting viewpoint pairs, as it avoids unnecessary rotation that can lead to VR sickness [12]. However, in our design, we also aim to avoid occlusion with scene objects (buildings in particular). Therefore, if a straight line trajectory is interrupted, we transform the path to a quadratic Bézier curve. The middle control point of the curve is determined by a vector rooted at a point off the coast or the further point that results in no intersection. Choosing a point off the coast is a preference expressed by domain experts so that while navigating, one may also get a chance to view how the impact of coastal flooding – synonymous with disaster analysis protocol undertaken by emergency managers. To reduce VR sickness due to sharp curvature [12], we set the vector length to be three times the distance between the center point and the straight line.

5 IMPLEMENTATION DETAILS

Submerge is developed using Unity 3D [44] game engine. The modular and drag-and-drop interface of Unity automatically provides an interactive framework for configuring and amending the individual components of Submerge listed in the previous section or adding new ones based on application needs. Moreover, using Unity AR Foundation [45] we are able to perform the localization on any auxiliary device, irrespective of the underlying operating system. In keeping up with the agnosticism of devices, we implement our remote rendering framework using the WebRTC package for Unity [46].

To set up the display system layout, we interactively define the physical width, height, and relative placement and orientation of the virtual screens using quads as a visual guide (see Fig. 6). A virtual screen is a canvas that can comprise either a single or multiple monitors, typically configured at the operating system or the GPU driver level. For each virtual screen, a set of attributes need to be configured, namely, for multi-node systems, its network address, and for multi-GPU systems, the GPU port number. Using these configurations, we can launch instances of Submerge on the respective display nodes for the respective virtual screens. A server application then connects to each client instance and performs its synchronization and interaction tasks in parallel, implemented using Unity’s networking protocol.

To ensure an interactive framerate, we perform the computations for both vertex height interpolation and wave generation, on the GPU using shaders. At the application startup and during the scene update, a triangular mesh with intervals equal to the quadnode length is generated. By initializing a coarse mesh on the CPU, we optimize the number of triangle draw calls on the GPU by performing hardware-level tessellation. To this end, we apply two tessellation passes on each triangle. For the first pass, we subdivide a triangle based on its distance from the camera. The tessellation factor is maximum when the camera is at a minimum defined distance from the water surface (e.g., our default value is 100 meters), and gradually decreases until

it reaches a maximum defined distance (e.g., our default value is 2000 meters). If the triangles in the initial mesh have largely varying edge lengths, the output from the distance-based tessellation pass will result in smaller triangles being tessellated more than larger triangles. Thus, in the second tessellation pass, we further refine the tessellated triangles in the camera frustum to have a maximum allowable edge length. Although we empirically set this value to be one-tenth of the smallest quadnode length, this can be changed based on available GPU resources.

A limitation of using height-field grids is that information is cell-centered rather than spatially localized. For new vertices generated during tessellation, it becomes challenging to check for intersections with other scene objects accurately. This is important to avoid rendering artifacts where the wave is only partially visible on the terrain. Thus, in our shader design, we cache the interpolated height of each vertex, along with its crest and trough heights, and perform a depth test using a depth buffer. Since the wave amplitude in our design is solely to induce a perception of the direction of flow and does not hold any numerical significance, we perform the following operations in the surface shader: (1) if the cached interpolated height is projected higher in the depth buffer than other scene objects and either the crest or trough is occluded, the amplitude is reduced to a minimal value (in our case, 1mm), (2) if the interpolated height is occluded in the depth buffer, it is shaded transparent.

6 RESULTS AND EVALUATION

We demonstrate Submerge for a simulated flooding scenario of superstorm Sandy impacting NYC [47], visualized on three kinds of display modalities: a single-screen desktop, a single-wall multi-GPU tiled-display setup (tiled-display), and the Stony Brook Reality Deck (RD), a room-sized 1.5 gigapixel-resolution immersive display facility. The specifications and layout for each display system are illustrated in Fig. 6(a)-(c), respectively. All three systems are equipped with NVIDIA Quadro RTX6000 GPU hardware and Intel Xenon 2.80GHz CPU with 128GB of RAM.

The flooding data is generated using the ADCIRC simulation model and spans the NYC area (302.6mi^2), containing $908,000$ datapoints \times 288 timepoints (30 mins interval). For constructing a NYC virtual scene, we used publically available datasets [48] to integrate a DEM, texture map it using the highest available resolution aerial NYC images [49], and 3D buildings. Consequently, for this scenario, Submerge managed a total data size of 15GB (excluding aerial textures which we directly streamed from the internet at runtime).

In terms of runtime performance, the startup time for the single-display, tiled-display, and RD, at the highest LoD, were 66s, 110s, and 145s, respectively. This accounts for 3D object loading, quadtree construction, and floodwater surface rendering. The texture mapping was performed in parallel, streamed directly from the internet, and therefore not included in the time performance. Once initialized, Submerge was able to synthesize and render the animated waves, at a framerate of 40 frames-per-second (fps). The inset (d) in Fig. 6 shows an example of waves synthesized using our approach, for a waterbody area in the scene.

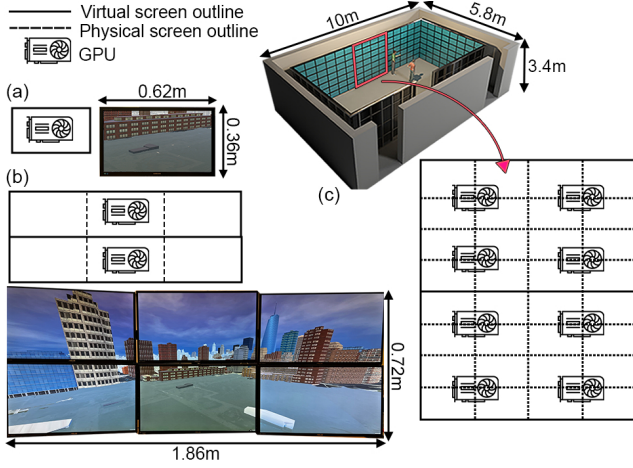


Fig. 6. We demonstrate Submerge on three display systems: (a) single-screen, (b) tiled-display, and (c) Reality Deck, a room-sized gigapixel immersive facility. Inset (d) shows a result of our wave synthesis and (e) illustrates the detail that can be resolved approaching the facility walls.

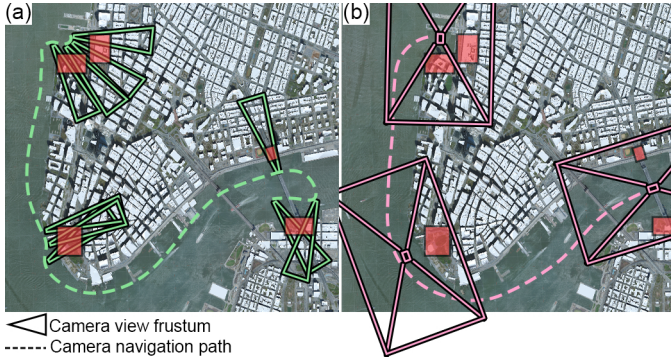


Fig. 7. Camera views and navigation path generated for (a) a single screen and (b) four-walled RD. The red boxes are user-marked POIs.

During manual scene navigation, updating the quadtree using our dynamic approach maintained 25-30 fps. However, navigating the scene automatically using our camera path algorithm did not affect the framerate, since the path is pre-calculated and the quadtree is updated preemptively in parallel, as the camera is moved along the path.

Three areas in NYC were of particular interest to our domain collaborators for analysis: the road and open space for a potential evacuation point next to the coast at the eastern side of Manhattan, the Battery park and tunnel area, and road infrastructure at both ends of a bridge on the western end of Manhattan. For the POIs marked using red boxes in Fig. 7, we show the results for our automatic camera viewpoints and path generation for the tiled-display RD in (a) and (b), respectively. Since the tiled-display is a single-screen setup with a relatively small FoV, we adjust the default weights for the viewpoint optimization such that the POI is positioned towards the center of the display ($\omega_u = 0.9$, $A = \pi/12$) and nearer to the camera ($\omega_d = 0.75$, $K = 500m$). Conversely, utilizing the very large FoV of the RD, we adjusted the weights such that the POI could be anywhere within the view of the four walls ($\omega_u = 0.1$, $A = \pi/6$), and enable comparison by allowing multiple POIs to be viewed at an instance ($\omega_d = 0.25$, $K = 1000m$). For both displays, 1000 particles were randomly initialized

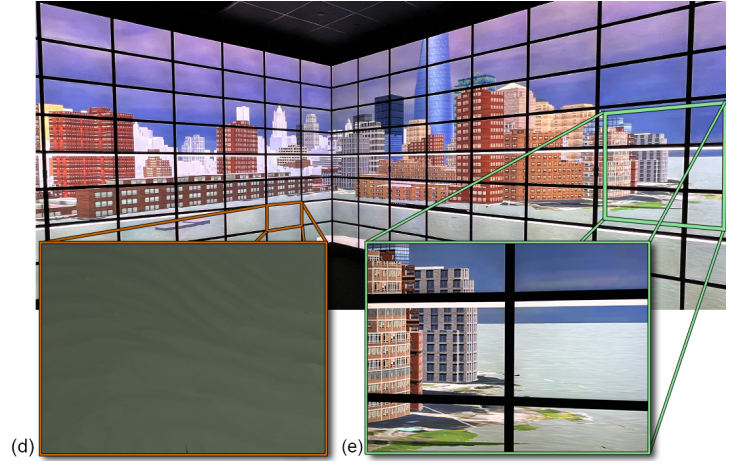


Fig. 8. Interaction with data in the RD can be performed either (a) naturally or (b) using our auxiliary display system.

for the PSO algorithm. It took 120s to determine camera views for the single display and 75s for the RD.

Finally, in Fig. 8 we demonstrate how users can explore the data by either performing natural pan-and-zoom interactions, as in Fig. 8(a), or the auxiliary display system to view additional contextual information, as shown in Fig. 8(b). Additionally, using a game controller, users can manually navigate the scene or use our automatic navigation path to view the marked POIs, and update the timepoint of the flooding scenario. Based on domain expert feedback, we have implemented the following visualization and interactions for focus+context on the auxiliary display:

Dip-stick metaphor: Although color and opacity transfer functions provide both, a qualitative and quantitative visual sense of the flooding depth, meteorologists additionally prefer to note quantitative measurement values. Desktop-based applications achieve this by providing a legend or designing a mouse-based tool-tip to display the depth value. To adopt a natural way of measuring depth, we render a ruled dip-stick on the auxiliary display, as shown in Fig. 8(b), that shows water markings on the measurements when the device is pointed to the water surface mesh.

Selection and occlusion removal for buildings: Since the auxiliary display can complement interaction metaphors such as selection, we provide users the ability to point and select a specific building to view additional information.

Fig. 8(c) demonstrates such an example where for a selected building, we change its color to represent the flooding level severity relative to its height (also see Fig. 5(a), and a label with information such as its name, location (address, along with latitude and longitude), and any additional related information provided by the user. Moreover, to enhance visibility, we remove scene objects and buildings that occlude the selected building in the auxiliary display camera view and in a radius around the building.

Visualizing additional contextual information: For any domain-specific additional data, we allow users to (1) select the 3D scene object class for which the data is to be visualized, namely, water surface mesh, 3D buildings, or a new plane spanning the scene extents, and (2) configure a transfer function for the rendering. Fig. 5(b) is an example of this feature, demonstrating a heatmap of NYC population density atop the flooding scenario.

6.1 Domain Expert Feedback

To evaluate our work and the effectiveness of using Submerge in an immersive setting, we conducted two workshop spaces, one specialized with domain experts and the other with college students without domain knowledge.

For the specialized workshop, we invited 10 participants with backgrounds in research and academia, NYC emergency managers, and National Weather Services (NWS). In following NWS protocol, an informational orientation of an upcoming storm was presented to the participants to imitate a situation where experts engage in preparedness ahead of a weather event. The identity of the storm simulation dataset was not revealed to the participants as it would have influenced their perception due to prior knowledge or memory. The participants were first asked to express and follow the steps they would have normally taken to analyze the provided information. Following that, they were collectively shown Submerge in the RD, for POIs marked in Fig. 7. All experts appreciated the visualizations presented to them. One unanimous comment was that the 3D visualization and sense of realism, coupled with immersion, positively transformed the way they planned for preparation, evacuation, and resilience measures, in contrast to currently adopted 2D methods. Specifically, the to-scale rendering aided them in having a clearer spatial perception of the flooding levels with respect to the surroundings, for instance, the buildings, streets, and open areas. To this end, the participants found most effective what they called the *street-view*, as shown in Fig. 8 and Fig. 9(a)-(c), as they could visualize the flood level with respect to their own height. One participant reflected that “the display of flooding in 3D with actual buildings was a much more effective method of communicating risks, rather than a numerical forecast or a 2D risk map.” Another participant commented that the visualizations in the RD felt like “a helicopter ride during a catastrophe where [they] get a wholesome view of the city, and then go down at street level to investigate its intensity.” Moreover, they expressed that the shared experience exploring the data allowed for greater insights as participants were able to instantaneously take into account the diversity of expertise and domains for their analysis and decisions. An example of this was witnessed when an atmospheric scientist explained to an

emergency manager how an incoming storm surge would result in a drastic increase in flooding levels of an area and thus may be considered a priority in evacuation plans.

Feedback from the first workshop enabled us to address some shortcomings, consequently directing us in conducting our research and developing the auxiliary display framework, automatic viewpoint and scene navigation, and synthesizing the tidal waves. We conducted a second specialized workshop with 10 students in atmospheric sciences, particularly emphasizing the new Submerge features. The auxiliary display was welcomed by the participants, especially since they could now make quantitative measurements and seamlessly integrate their domain data visualization for personal-level analysis as well as share their findings collaboratively. *Occlusion removal* was often utilized to get a clearer view of the surrounding landscape and road network. Compared to manual navigation, all participants preferred the automatic camera views and navigation. At some instances, participants requested to change the camera views for exploring the area around the POI. A few participants however experienced VR sickness during the navigation and one suggested that they would have preferred an instant scene change from one POI to the next. Finally, the participants greatly acknowledged wave synthesis for flow direction. Results from Fig. 9(a)-(c), the Battery Tunnel area, were of a particular learning experience. For each incremental timepoint, the participants were able to observe, for the first time, how tidal surge from different directions contributed to the increasing flooding levels in the area. This information was not perceivable otherwise using a still water surface mesh rendering.

A separate workshop with 80 college students was conducted to evaluate the impact of standard weather forecasting graphics compared to Submerge visualizations. Following a pre-recorded narration of a storm weather forecast, the participants were presented with a hurricane flooding scenario for a fictitious college campus. We deployed Submerge on a single-screen desktop setting, without an auxiliary display. In terms of taking action in favor of preparedness, participants agreed that the visualizations aided their decision-making. A comment by a participant that led to general consensus was that the ability to “see” the flooding, which would otherwise be narrated using words, such as “we are expecting 3-5 feet of storm surge flooding,” or 2D graphs, not only allowed them to understand the forecast severity but also made them more likely to avoid that situation.

7 CONCLUSION AND FUTURE WORK

We have presented Submerge, an application for visualizing flooding scenarios rendered in 3D using numerical simulation and GIS data, along with a scalable framework for deploying the application in custom immersive display systems. For rendering the flooding level, we have developed a real-time approach that constructs a smooth surface mesh, coupled with animated tidal waves to depict the flooding direction. We achieve this by constructing a dynamic quadtree datastructure that interactively updates based on the camera view frustum and is utilized to implement an adaptive grid for sampling and interpolation of the mesh height values and wave direction. Specifically for

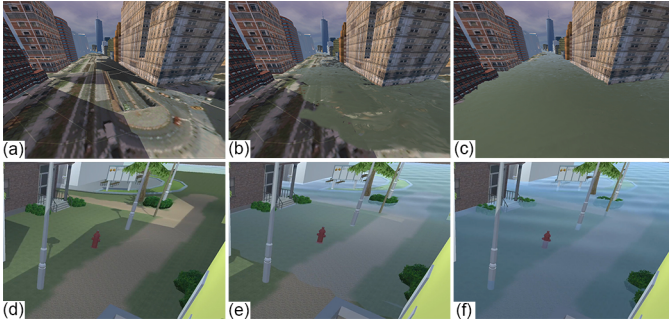


Fig. 9. Scenes from the specialized workshop showing NYC in (a)-(c), and the college workshop showing a fictitious scene in (d)-(f). For both, we show no flooding, mid-level, and maximum flooding, respectively.

immersive visual systems, we have introduced two novel interaction modalities: an automatic camera view-finding and path-generation algorithm, and an AR-based auxiliary display system. We find optimal camera views for marked POIs based on the screen layout and viewing parameters of the POI with respect to the layout. For traversing through the views, our path-generation algorithm is designed to avoid collision and reduce VR-sickness, while also facilitating effective scene exploration during the navigation. The auxiliary display is a unique design that compliments the visualizations on the shared screen space by displaying additional contextual information about the virtual scene, using AR. The resulting visualizations and particularly the utility of an immersive display system have been positively evaluated by domain experts and other stakeholders.

Based on feedback received during evaluation, we identified a limitation that while Submerge enhances a sense of realism, it does not fully achieve the features of a decision system. Therefore, for future work, we plan to integrate tools that will allow stakeholders to visualize outcomes by interactively applying scenarios for mitigation and evacuation measures. Moreover, one natural limitation of large immersive facilities is their immobile nature. To this end, we plan to extend the Submerge system to support VR HMDs and include a framework for co-located as well as remote collaboration across all devices. Finally, we aim to conduct further research to extend the Submerge visualization and system framework for stereo display systems.

ACKNOWLEDGMENTS

This project was supported in part by NSF grants CNS1650499, OAC1919752, ICER1940302, and IIS2107224.

REFERENCES

- [1] C. B. Field, V. R. Barros, M. D. Mastrandrea, K. J. Mach, M.-K. Abdurabo, N. Adger, Y. A. Anokhin, O. A. Anisimov, D. J. Arent, J. Barnett *et al.*, "Summary for policymakers," in *Climate change 2014: impacts, adaptation, and vulnerability*. Cambridge University Press, 2014, pp. 1–32.
- [2] "DAT: The International Disasters Database," <https://www.emdat.be/>, accessed: 2022-02-25.
- [3] A. H. Murphy, "What is a good forecast? an essay on the nature of goodness in weather forecasting," *Weather and Forecasting*, vol. 8, no. 2, pp. 281–293, 1993.
- [4] D. Cornel, A. Konev, B. Sadransky, Z. Horvath, E. Gröller, and J. Waser, "Visualization of object-centered vulnerability to possible flood hazards," *Comp. Graph Forum*, vol. 34, no. 3, pp. 331–340, 2015.
- [5] D. Cornel, A. Buttinger-Kreuzhuber, A. Konev, Z. Horvath, M. Wimmer, R. Heidrich, and J. Waser, "Interactive visualization of flood and heavy rain simulations," *Comp. Graph Forum*, vol. 38, no. 3, pp. 25–39, 2019.
- [6] R. Ball and C. North, "Realizing embodied interaction for visual analytics through large displays," *Computers & Graphics*, vol. 31, no. 3, pp. 380–400, 2007.
- [7] C. Andrews, A. Endert, B. Yost, and C. North, "Information visualization on large, high-resolution displays: Issues, challenges, and opportunities," *Info. Vis.*, vol. 10, no. 4, pp. 341–355, 2011.
- [8] B. Laha, K. Sensharma, J. D. Schiffbauer, and D. A. Bowman, "Effects of immersion on visual analysis of volume data," *IEEE Trans Vis Comput Graph*, vol. 18, no. 4, pp. 597–606, 2012.
- [9] J. M. Mol, W. W. Botzen, and J. E. Blasch, "After the virtual flood: Risk perceptions and flood preparedness after virtual reality risk communication," *Judgm. Decis. Mak.*, vol. 17, no. 1, p. 189, 2022.
- [10] B. Kim and P. Tsiotras, "Image segmentation on cell-center sampled quadtree and octree grids," *Wavelet Applications in Industrial Processing VI*, vol. 7248, pp. 139–147, 2009.
- [11] X. Bonaventura, M. Feixas, M. Sbert, L. Chuang, and C. Wallraven, "A survey of viewpoint selection methods for polygonal models," *Entropy*, vol. 20, no. 5, p. 370, 2018.
- [12] P. Hu, Q. Sun, P. Didyk, L.-Y. Wei, and A. E. Kaufman, "Reducing simulator sickness with perceptual camera control," *ACM Trans. Graph.*, vol. 38, no. 6, p. Article 210, Nov. 2019.
- [13] C. Papadopoulos, K. Petkov, A. E. Kaufman, and K. Mueller, "The Reality Deck—an Immersive Gigapixel Display," *IEEE Computer Graphics and Applications*, vol. 35, no. 1, pp. 33–45, 2015.
- [14] J. G. Leskens, C. Kehl, T. Tutenel, T. Kol, G. d. Haan, G. Stelling, and E. Eisemann, "An interactive simulation and visualization tool for flood analysis usable for practitioners," *Mitigation & Adaptation Strategies for Global Change*, vol. 22, no. 2, pp. 307–324, 2017.
- [15] National Oceanic and Atmospheric Administration, "Sea Level Rise Viewer," <https://coast.noaa.gov/slr/#>, accessed Oct 26, 2022.
- [16] D. Leedal, J. Neal, K. Beven, P. Young, and P. Bates, "Visualization approaches for communicating real-time flood forecasting level and inundation information," *Journal of Flood Risk Management*, vol. 3, no. 2, pp. 140–150, 2010.
- [17] M. Vuckovic, J. Schmidt, T. Ortner, and D. Cornel, "Combining 2D and 3D Visualization with Visual Analytics in the Environmental Domain," *Information*, vol. 13, no. 1, p. 7, 2021.
- [18] N. Lipp, N. Dużmańska-Misiarczyk, A. Strojny, and P. Strojny, "Evoking emotions in VR: schema activation via a freeze-frame stimulus," *Virtual Reality*, vol. 25, no. 2, pp. 279–292, 2021.
- [19] K. Kroesl, H. Steinlechner, J. Donabauer, D. Cornel, and J. Waser, "Master of Disaster: Virtual-Reality Response Training in Disaster Management," *ACM International Conference on Virtual-Reality Continuum and its Applications in Industry*, 2019.
- [20] M. T. Oyshi, V. Maleska, J. Schanze, F. Bormann, R. Dachsel, and S. Gumhold, "Floodvis: Visualization of climate ensemble flood projections in virtual reality," *EG Workshop on Visualisation in Environmental Sciences*, pp. 27–359, 2022.
- [21] P. Reipschlag, T. Flemisch, and R. Dachsel, "Personal augmented reality for information visualization on large interactive displays," *Transactions on Visualization and Computer Graphics*, vol. 27, no. 2, pp. 1182–1192, 2020.
- [22] S. Chen, H. Wu, Z. Lin, C. Guo, L. Lin, F. Hong, and X. Yuan, "Photo4action: phone camera-based interaction for graph visualizations on large wall displays," *Journal of Visualization*, vol. 24, no. 5, pp. 1083–1095, 2021.
- [23] A. Nishimoto and A. E. Johnson, "Extending virtual reality display wall environments using augmented reality," in *Symposium on Spatial User Interaction*, 2019, pp. 1–5.
- [24] J. Davis and X. Chen, "Lumipoint: Multi-user laser-based interaction on large tiled displays," *Displays*, vol. 23, no. 5, pp. 205–211, 2002.
- [25] C. Ganser, A. Steinemann, and A. Kunz, "Infractables: Multi-user tracking system for interactive surfaces," in *IEEE Virtual Reality Conference*, 2006, pp. 253–256.
- [26] R. Langner, U. Kister, and R. Dachsel, "Multiple coordinated views at large displays for multiple users: Empirical findings on user behavior, movements, and distances," *IEEE Trans Vis Comput Graph*, vol. 25, no. 1, pp. 608–618, 2018.
- [27] M. R. Morris, A. Huang, A. Paepcke, and T. Winograd, "Cooperative gestures: multi-user gestural interactions for co-located groupware," *ACM CHI*, pp. 1201–1210, 2006.

- [28] S. Malik, A. Ranjan, and R. Balakrishnan, "Interacting with large displays from a distance with vision-tracked multi-finger gestural input," *ACM UIST*, pp. 43–52, 2005.
- [29] J. O. Wobbrock, M. R. Morris, and A. D. Wilson, "User-defined gestures for surface computing," *ACM CHI*, pp. 1083–1092, 2009.
- [30] S. Siddhupuria, S. Malacria, M. Nancel, and E. Lank, "Pointing at a distance with everyday smart devices," *ACM CHI*, pp. 1–11, 2018.
- [31] T. Babic, H. Reiterer, and M. Haller, "Understanding and creating spatial interactions with distant displays enabled by unmodified off-the-shelf smartphones," *Multimodal Technologies and Interaction*, vol. 6, no. 10, p. 94, 2022.
- [32] R. Langner and R. Dachsel, "Towards visual data exploration at wall-sized displays by combining physical navigation with spatially-aware devices," in *IEEE VIS Poster*, 2018.
- [33] T. Kamada and S. Kawai, "A simple method for computing general position in displaying three-dimensional objects," *Computer Vision, Graphics, and Image Processing*, vol. 41, no. 1, pp. 43–56, 1988.
- [34] M. Feixas, E. Del Acebo, P. Bekaert, and M. Sbert, "An information theory framework for the analysis of scene complexity," *Computer Graphics Forum*, vol. 18, no. 3, pp. 95–106, 1999.
- [35] T. Arbel and F. P. Ferrie, "Viewpoint selection by navigation through entropy maps," *IEEE Intl Conf. Computer Vision*, vol. 1, pp. 248–254, 1999.
- [36] P.-P. Vázquez, M. Feixas, M. Sbert, and W. Heidrich, "Viewpoint selection using viewpoint entropy," *Sixth International Fall Workshop on Vision, Modeling, and Visualization*, pp. 273–280, 2001.
- [37] S. L. Stoev and W. Straßer, "A case study on automatic camera placement and motion for visualizing historical data," *IEEE Visualization*, pp. 545–548, 2002.
- [38] H. Huang, D. Lischinski, Z. Hao, M. Gong, M. Christie, and D. Cohen-Or, "Trip synopsis: 60km in 60sec," *Computer Graphics Forum*, vol. 35, no. 7, pp. 107–116, 2016.
- [39] L. Lin, Y. Liu, Y. Hu, X. Yan, K. Xie, and H. Huang, "Capturing, reconstructing, and simulating: the UrbanScene3D dataset," *European Conference on Computer Vision*, pp. 93–109, 2022.
- [40] Q. Liang, "A structured but non-uniform Cartesian grid-based model for the shallow water equations," *International Journal for Numerical Methods in Fluids*, vol. 66, no. 5, pp. 537–554, 2011.
- [41] D. Hinsinger, F. Neyret, and M.-P. Cani, "Interactive animation of ocean waves," *EG Symp on Computer Animation*, pp. 161–166, 2002.
- [42] S. Thon, J.-M. Dischler, and D. Ghazanfarpour, "Ocean waves synthesis using a spectrum-based turbulence function," *IEEE Proceedings Computer Graphics International*, pp. 65–72, 2000.
- [43] J. Kennedy and R. Eberhart, "Particle swarm optimization," in *International Conf. on Neural Networks*, vol. 4, 1995, pp. 1942–1948.
- [44] Unity Technologies, "Unity3D," <https://unity3d.com/unity/>.
- [45] Unity, "Unity ar foundation," <https://unity.com/unity/features/arfoundation>, online; accessed Oct 26, 2022.
- [46] Unity, "WebRTC for Unity," <https://github.com/unity-technologies/com.unity.webrtc>, accessed Oct 26, 2022.
- [47] B. A. Colle, M. J. Bowman, K. J. Roberts, M. H. Bowman, C. N. Flagg, J. Kuang, Y. Weng, E. B. Munsell, and F. Zhang, "Exploring water level sensitivity for metropolitan new york during sandy (2012) using ensemble storm surge simulations," *Journal of Marine Science and Engineering*, vol. 3, no. 2, pp. 428–443, 2015.
- [48] NYC Planning, "NYC BYTES of the BIG APPLE," <https://www.nyc.gov/site/planning/data-maps/open-data.page>, online; accessed Oct 26, 2022.
- [49] Open Street Maps, "Open StreetMap," https://wiki.openstreetmap.org/wiki/Main_Page, accessed Oct 26, 2022.



Saeed Boorboor is currently pursuing a Ph.D. degree in Computer Science at Stony Brook University. He received his Bachelor degree in Computer Science from School of Science and Engineering, Lahore University of Management Sciences, Pakistan. His research interests include scientific visualization, medical imaging, and computer graphics.



Yoonsang Kim is currently pursuing a Ph.D. degree in Computer Science at Stony Brook University. He received his Bachelor's degree in Computer Science from Soongsil University, South Korea, and Master's degree in Computer Science from Stony Brook University. His research interests include augmented reality, virtual reality, data visualization, computer graphics, and human-computer interaction.



Ping Hu is currently pursuing a Ph.D. degree in Computer Science at Stony Brook University. She received her Bachelor degree of Physics at Shandong University, China. Her research focuses on computational camera control in scientific visualization and computer graphics.



Josef Moses is currently pursuing a Bachelor degree and Master degree in Atmospheric Science at Stony Brook University. His research interests include meteorology, risk communication, severe weather communication, and social science.



Sciences from the University of Washington (1997).

Brian A. Colle is a Professor of Atmospheric Sciences and the Division Head for the Atmospheric Sciences Division (2018-present) at Stony Brook University, School of Marine and Atmospheric Sciences (SoMAS). He has published over 125 papers during the last 25 years on various aspects of extreme weather and climate, including the application and improvement of weather prediction models for these events. He is a Fellow of the American Meteorological Society. He received his Ph.D. in Atmospheric



National Academy of Inventors Fellow, recipient of IEEE Visualization Career Award (2005), and inducted into Long Island Technology Hall of Fame (2013) and IEEE Visualization Academy (2019). He received his Ph.D. in Computer Science from Ben-Gurion University, Israel (1977).

Arie E. Kaufman is a Distinguished Professor of Computer Science, Director of Center of Visual Computing, and Chief Scientist of Center of Excellence in Wireless and Information Technology at Stony Brook University. He served as Chair of Computer Science Department, 1999-2017. He has conducted research for >40 years in visualization, VR and graphics and their applications, and published >350 refereed papers. He was the founding Editor-in-Chief of IEEE TVCG, 1995-98. He is an IEEE Fellow, ACM Fellow,